

CALCAREOUS PLANKTON BIOSTRATIGRAPHY OF THE SANTONIAN-CAMPANIAN BOUNDARY INTERVAL IN THE BOTTACCIONE SECTION (UMBRIA-MARCHE BASIN, CENTRAL ITALY)

FRANCESCO MINIATI, MARIA ROSE PETRIZZO, FRANCESCA FALZONI & ELISABETTA ERBA*

Dipartimento di Scienze della Terra “Ardito Desio”, Università degli Studi di Milano, Via Mangiagalli 34, 20133 Milano, Italy.

*Corresponding author. E-mail: elisabetta.erba@unimi.it

To cite this article: Miniati F., Petrizzo M.R., Falzoni F. & Erba E. (2020) - Calcareous plankton biostratigraphy of the Santonian-Campanian boundary interval in the Bottaccione Section (Umbria-Marche Basin, Central Italy). *Riv. It. Paleontol. Strat.*, 126(3): 771-789.

Keywords: Calcareous nannofossils; planktonic foraminifera; biostratigraphy; Santonian-Campanian boundary.

Abstract: The Bottaccione section (Umbria-Marche Basin, central Italy) was analyzed for calcareous nannofossil and planktonic foraminiferal biostratigraphy across the Santonian-Campanian boundary interval to achieve a high-resolution and updated zonation directly calibrated with magnetostratigraphy. Several calcareous plankton events were detected, including zonal markers and additional potential biohorizons. The base of magnetochron C33r, proposed for placement of the base of the Campanian, lies between the first occurrence of *Aspidolithus parvus parvus* and the last occurrence of *Dicarinella asymetrica* in the Bottaccione section. The literature survey indicates that these events were found in the Santonian-Campanian boundary interval at supraregional scale and, may be used to confidently approximate the base of the Campanian.

INTRODUCTION

The Bottaccione section, located near the city of Gubbio in central Italy (coordinates: 43°21'56.05" N, 12°34'57.56" E; Fig. 1), consists of a continuous Jurassic to Paleocene pelagic sequence deposited in the Umbria-Marche Basin (central-western Tethys). The portion of the Bottaccione section investigated in this study is entirely comprised in the Scaglia Rossa Formation and is exposed in the Bottaccione Gorge. The Scaglia Rossa Formation spans from the lower Turonian to the middle Eocene (e.g., Arthur & Fischer 1977; Cresta et al. 1989) and consists of pink to red pelagic limestone that is a lithified

nannofossil-planktonic foraminiferal ooze, deposited at some 1500 m paleodepth (Arthur & Premoli Silva 1982). Bedding thickness ranges from 10 to 30 cm with common stylolites in the thicker beds. The Cretaceous Scaglia Rossa is divided in two members, the lower R1 member (Turonian-lower Campanian) is characterized by chert nodules and layers and the upper R2 member (lower Campanian-Maastrichtian) is predominantly made of pink to red-brown limestone without chert (Alvarez & Montanari 1988). The Bottaccione sequence represents a reference section used also in the Geologic Time Scale (GTS2012, Gradstein et al. 2012) for the Late Cretaceous.

We investigated calcareous nannofossils and planktonic foraminifera across the uppermost San-

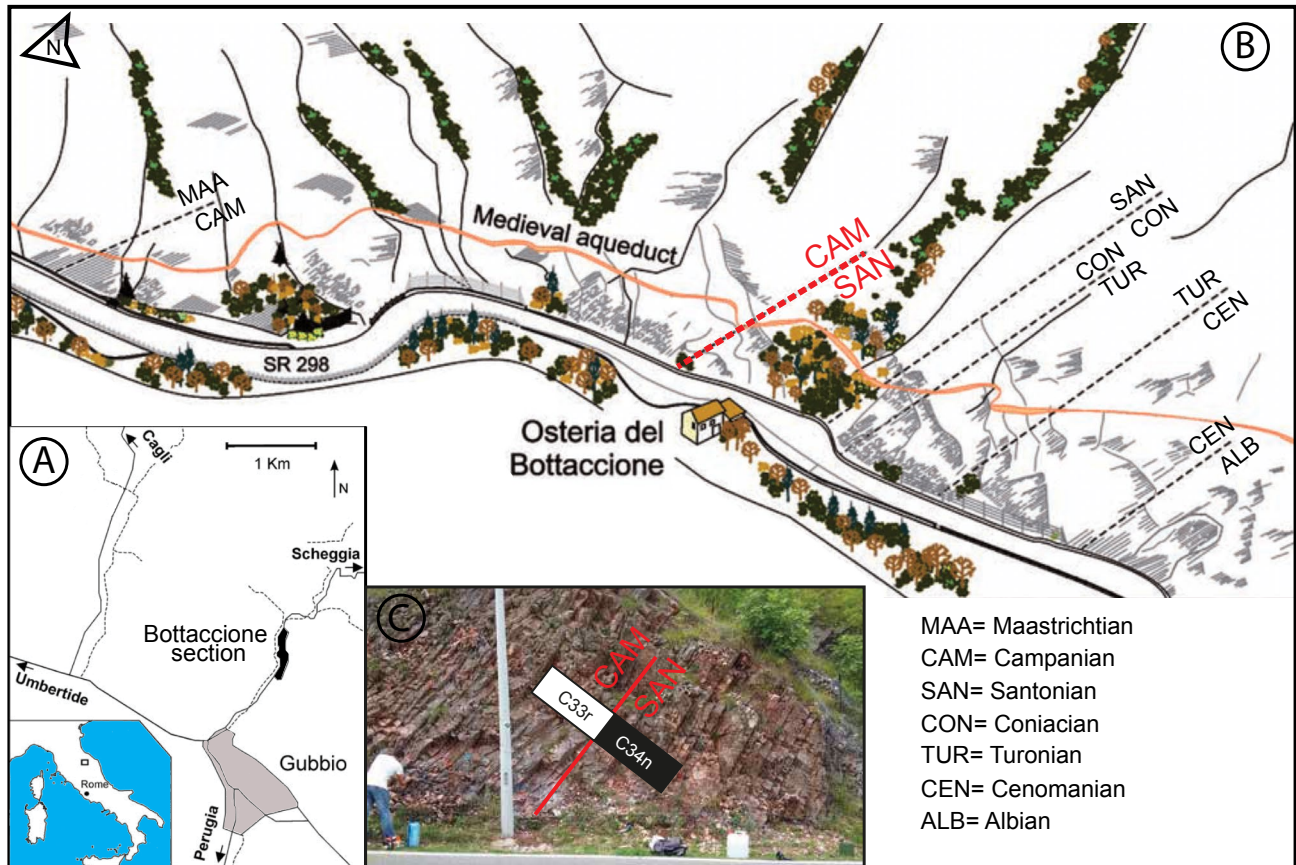


Fig. 1 - A) Location of the Bottaccione section. B) Schematic picture of the outcrop. The dashed lines indicate the position of the stage boundaries along the succession, the Santonian-Campanian boundary is in red (modified after Coccioni & Premoli Silva 2015). C) Photograph of the outcrop across the C34n/C33r magnetostratigraphic boundary at 221.525 ± 0.075 m (after Maron & Muttoni, accepted).

tonian to lowermost Campanian interval, within the lower R1 member. The Bottaccione section has been appointed as a candidate for the Campanian Global Stratotype Section and Point (GSSP) and revised/updated calcareous plankton biostratigraphy is meant to concur to the integrated characterization of the Santonian-Campanian boundary interval (minutes ISCS meeting at Strati 2019, <http://cretaceous.stratigraphy.org/archives/>). Following the suggestion by the Campanian Working Group of the International Subcommittee on Cretaceous Stratigraphy (see minutes of the ISCS meeting at Strati 2019, <http://cretaceous.stratigraphy.org/archives/>), the base of the Campanian Stage is placed at the base of magnetic Chron 33r that in the Bottaccione section falls at 221.60 m according to the detailed paleomagnetic study by Maron & Muttoni (accepted). As described by Maron & Muttoni (accepted) a negligible fault, with a few decimeters-displacement, occurs at 221.20 m: the lithostratigraphy has been controlled in detail and proved to be con-

tinuous. The calcareous plankton biostratigraphy is directly calibrated with polarity magnetozones (Maron & Muttoni, accepted) to improve, revise and/or consolidate the integrated bio-magnetostratigraphy of the Santonian-Campanian boundary interval (Premoli Silva & Sliter 1995; Gardin et al. 2001; Tremolada 2002; Petrizzo et al. 2011; Coccioni & Premoli Silva 2015).

MATERIAL AND METHODS

Calcareous nannofossils

A total of 45 samples were analyzed for calcareous nannofossil biostratigraphy in the interval from meter 211 to meter 233 (Premoli Silva & Sliter 1995) across the Santonian-Campanian boundary (Fig. 3) using subsamples of magnetostratigraphy samples. An average sampling resolution of 0.50 cm was applied, but sampling resolution was increased to 0.10 cm between 220 m and 221 m (across the C34n/C33r magnetic polarity boundary).

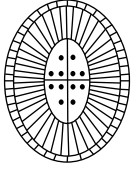
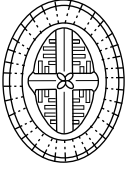
Family		Arkhangelskiellaceae	
Genus		<i>Aspidolithus</i>	<i>Broinsonia</i>
Schematic sketch (not in scale)			
Margin		Bicyclic (Radial)	Bicyclic (Radial)
Central area structures	Cross	No	Yes
	Plates	Yes	No
	Perforations	Yes	No

Fig. 2 - Illustration of diagnostic characters (distal view) for separating genera *Aspidolithus* and *Broinsonia*.

Samples were prepared as simple smear slide following the standard preparation techniques (Monechi & Thierstein 1985). Each sample was analyzed using a polarizing microscope at 1250X magnification, investigating 6 full traverses (= 1000 fields of view). Semiquantitative data were achieved for total nannofossil and individual taxa abundances and preservation characterized based on the degree of overgrowth and/or dissolution (Suppl. Tab. 1). The biostratigraphy was conducted following the zonations of Sissingh (1977) as modified by Perch-Nielsen (1985), Roth (1978), Bralower et al. (1995) and Burnett (1998) applying the CC, NC, NC* and UC codes, respectively.

Morphometric data were acquired for *Aspidolithus parvus* subspecies using pictures captured with a Q-imaging Micropublisher 5.0 RTV camera (Q-capture Prosuite software) mounted on a Leitz Laborlux light microscope. Measurements were obtained using the Image J64 software, with an error of $\pm 0.08 \mu\text{m}$.

Planktonic foraminifera

Planktonic foraminifera were studied by integrating thin sections and washed residues obtained from the samples used for magnetostratigraphy (Maron & Muttoni, accepted). A total of 33 samples were studied in thin sections and 19 sample out of 33 were also studied in washed residues (Suppl. Tab. 2) which were obtained by processing about 80-100 g of rock samples with acetic acid (see pro-

cedure in Lirer 2000 and Falzoni et al. 2016). Santonian-Campanian limestones of the Scaglia Rossa Formation contain cherts that are particularly indurated and, as a consequence, rock samples were immersed in acetic acid for several hours to be disaggregated resulting in the common occurrence of broken or corroded specimens not identifiable at species level. Therefore, because of the poor preservation of planktonic foraminifera in the washed residues, only 19 samples were used for biostratigraphic analyses as they contained sufficiently well-preserved specimens to ensure reliable identification at species level.

Relative abundance data of planktonic foraminifera were collected for thin sections by screening the entire surface of the thin section (Suppl. Tab. 2). Planktonic foraminifera in the washed residues were studied on the $>63 \mu\text{m}$ size fraction and because of the generally poor preservation of the assemblages only the occurrence of species is reported in Supplementary Table 2.

Taxonomic concepts for planktonic foraminiferal species identification follow their original descriptions and illustrations, Premoli Silva & Sliter (1995), Petrizzo et al. (2011), Haynes et al. (2015) and the online taxonomic database for Mesozoic Planktonic Foraminifera “PF@mikrotax” available at <http://www.mikrotax.org/pforams/index.html> (see Huber et al. 2016). Biozonation is according to Premoli Silva & Sliter (1995) and Robaszynski & Caron (1995).

TAXONOMIC REMARKS

Calcareous nannofossils

The investigated interval is characterized by the evolution of two important lineages, namely of genera *Arkhangelskiella* and *Aspidolithus*. Changes in coccolith morphometry are used to separate different species that are biostratigraphically relevant in the Upper Cretaceous. Following Burnett (1997), within the genus *Arkhangelskiella* we grouped the specimens $<8 \mu\text{m}$ into *A. confusa* and specimens $>8 \mu\text{m}$ into *A. cymbiformis* (Pl. 1).

The *Aspidolithus* genus is differentiated here from genus *Broinsonia* as the latter is characterized by the presence of a cross instead of plates in the central area (Lauer 1975; Prins in Perch Nielsen 1979; Perch-Nielsen 1985). Bukry (1969) intro-

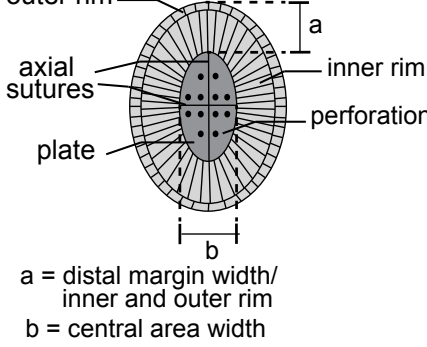

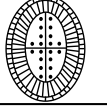
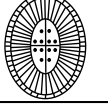
<i>Aspidolithus</i> terminology 	<i>Aspidolithus parvus</i> subspecies	Schematic sketch (not in scale)	central area (b) / distal margin (a) ratio	Dimensions holotype (µm)	
				length	width
	<i>A. parvus constrictus</i>		$b/a \leq 1$	10.6	8.3
	<i>A. parvus expansus</i>		$b/a \geq 2$	9.5	6.2
	<i>A. parvus parvus</i>		$1 < b/a < 2$	12.2	9.4

Fig. 3 - Schematic morphological characters (distal view) and their terminology of *Aspidolithus* specimens. *Aspidolithus parvus* subspecies are typified by the b (central area width)/a (distal margin width) ratio. The dimensions of length and width of the holotypes are reported.

duced the genus *Broinsonia* and selected *Broinsonia dentata* as type species. According to the original description, *B. dentata* is characterized by a central area divided by axial crossbars. The genus *Aspidolithus* was originally defined by Noël (1969) who indicated *Aspidolithus angustus* as type species. The holotype of *Aspidolithus angustus* (Noël 1969, Pl.1, figs 1a-c) is characterized by a central area filled by plates.

Lauer (1975) kept genera *Broinsonia* and *Aspidolithus* separated, but Veerbek (1977) and Hattner et al. (1980) considered them to be synonymous, *Broinsonia* having priority. Perch-Nielsen (1979), incorporating observations by Prins (personal communication in Perch-Nielsen 1979), returned to a differentiation of the two genera, due to presence of a distinct central cross in *Broinsonia* and perforated segments closing the central area in *Aspidolithus*.

Crux (1982) considered the genus *Aspidolithus* a junior synonym of *Broinsonia* and rejected the distinction between the two genera proposed by Perch Nielsen (1979) for various reasons: a) both Burky (1969) and Noël (1969) included in *Broinsonia* and *Aspidolithus*, respectively, forms with plates closing the central area as well as forms with a central cross; b) the margin structure (bicyclic) is the same in the two genera and considered highly diagnostic; c) poor preservation obliterates original characteristics of the central area, often producing apparent (but not real) crosses as a result of advanced etching of the plates. Analogously, *Aspidolithus* was disregarded by Bralower and Sissier (1992), Wise (1983), Burnett (1998) and Wolfgring et al. (2018).

Similarly to Almogi-Labin et al. (1991), Gardin et al. (2001), Tremolada (2002), we follow the diagnostic taxonomic characters synthesized by Perch-Nielsen (1985; Fig 14, p. 352) and, accordingly, maintain the distinction between *Broinsonia* and *Aspidolithus* as illustrated in Figure 2.

Within the *Aspidolithus* lineage, the subsequent appearances of *A. parvus expansus*, *A. parvus parvus* and *A. parvus constrictus* are marked by a gradual reduction of the central area/margin ratio as described by Wise (1983). We follow and apply the indications of Wise (1983) as illustrated in Figure 3.

Specimens of *Aspidolithus parvus* are characterized by changes in the central area/margin ratio, as well as by a variability in the coccolith length. An increase in coccolith length from smaller early specimens to larger later specimens of *Aspidolithus parvus* was observed by Bralower and Sissier (1982) and Almogi-Labin et al. (1991). Conversely, at the Falkland Plateau Wise (1983) did not observe any increase in the length of *Aspidolithus parvus* specimens.

In the Bottaccione section, Gardin et al. (2001) distinguished two morphogroups within the *Aspidolithus parvus* subspecies characterized by a total length <10 µm named as *A. parvus expansus* "small" and *A. parvus parvus* "small". According to Gardin et al. (2001) the small specimens of *A. parvus* have a distinct stratigraphic distribution compared to larger morphotypes. Similarly, at Postalm, Wolfgring et al. (2018) recognized five morphotypes within *Aspidolithus parvus* according to the b/a ratio and coccolith length. The *Aspidolithus* speci-

mens characterized by a length $<9\ \mu\text{m}$ (usually 6–8 μm) were placed within the species *Aspidolithus enormis*, as *A. enormis* sp.1 (b/a ratio ≥ 2) and *A. enormis* sp. 2 (b/a ratio < 2). Based on coccolith size, Wolfgring et al. (2018) assigned specimens of *Aspidolithus* with a length $>9\ \mu\text{m}$ (usually $>10\ \mu\text{m}$) to *A. parvus expansus* (b/a ratio ≥ 2), *A. parvus parvus* (b/a ratio between 1 and 2) and *A. parvus constrictus* (b/a ratio < 1).

Here, we apply the criteria of Gardin et al. (2001) to divide the small from the large morphogroups within genus *Aspidolithus*. Further details on the subspecies subdivisions are discussed in the Appendix.

Planktonic foraminifera

Taxonomic remarks are provided for some taxa in order to clarify the taxonomic concept applied in this study (Suppl. Tab. 2). The supra-specific classification of biserial taxa follows Haynes et al. (2015). The biserial *Sigalia* specimens observed in thin section and not identifiable at species level because only observed in edge view, were assigned to *Sigalia* sp. Multiserial specimens with depressed intercameral sutures and identified in edge view in thin sections were not classified at species level and thus assigned to *Ventilabrella* sp. The multiserial *Ventilabrella alpina*, a species largely overlooked in the literature and often regarded as a junior synonym of either *V. eggeri* (Nederbragt, 1991) or *V. multicamerata* (<http://www.mikrotax.org/pforams/index.html>), has been confidently identified in the studied assemblages.

The genus “*Globigerinelloides*” is quoted in the text and in the distribution chart (Suppl. Tab. 2) because it is polyphyletic and currently under taxonomic revision (see taxonomic notes in Petrizzo et al. 2017).

Very small-sized and/or poorly preserved hedbergellids not identifiable at species level were assigned to *Muricohedbergella* sp. Specimens here assigned to *Muricohedbergella delrioensis* s.l. usually possess 5 chambers in the last whorl, a moderate to fast chamber size increasing rate in the last whorl and include morphotypes showing a full range of morphologic variability between the neotypes designated by Longoria (1974) and by Masters (1976) (see Petrizzo & Huber 2006). Globigeriniform morphotypes with a thick wall resembling that shown by *Whiteinella*, *Rugoglobigerina* and *Costellagerina* species were identified in thin section only, however the observed cuts did not allow discrimination among these genera.

RESULTS

Calcareous nannofossils

The preservation of calcareous nannofossil assemblages in the studied interval ranges from moderate to poor with the presence of both overgrowth and etching. The total nannofossil abundances vary from common to rare with a higher abundance in the upper part of the studied interval (Suppl. Tab. 1). The assemblages are dominated by genera *Watznaueria*, *Eiffellithus* and *Retecapsa* as well as by the species *Cribrosphaerella ehrenbergii*. Marker and additional species are illustrated in Plates 1 and 2. Five bioevents were detected within the Santonian-Campanian boundary interval of the Bottaccione section (Fig. 3), allowing the identification of the CC17-CC18 zones of Sissingh (1977), NC17-NC18 zones of Roth (1978), NC17*-NC18a* zones of Bralower et al. (1995) and UC12 to UC14b zones of Burnett (1998).

The first occurrence (FO) of *Arkhangel'skiella cymbiformis* was observed at 219.10 m where the base of the UC13 zone was placed. All the observed specimens have a rim width $>1\ \mu\text{m}$, in contrast to what originally reported by Burnett (1997) for *A. cymbiformis*.

The FO of *Aspidolithus parvus parvus* at 220.5 m defines the base of the CC17, NC17, NC17* and UC14 zones. In the Bottaccione section, *A. parvus parvus* is extremely rare and discontinuous at the beginning of its range, becoming continuous and frequent from 224.6 m upwards: we labeled this change as first common occurrence (FCO) in this study. The FO of *Aspidolithus parvus constrictus* was detected at 229 m where the base of the UC14b subzone of Burnett (1998) was placed.

In the lower part of its range (between 220.5 and 225.75 m), the length dimensions of *A. parvus parvus* vary between 10 μm and 10.2 μm , with a single specimen of 9.6 μm in length at 221.3 m. According to Gardin et al. (2001), therefore, the older specimens are in the size range of *A. parvus parvus* ($\geq 10\ \mu\text{m}$) although very close to the lower limit of size range. A relative increase in length size ($>10.5\ \mu\text{m}$) of *A. parvus parvus* coccoliths is observed from 226.55 m upwards; these specimens co-occur with small and normal *A. parvus parvus* coccoliths with length varying from 8.4 to 11.7 μm . The presence of “small” *A. parvus parvus* was noted up to 232.85 m in the early Campanian. Our data indicate a gen-

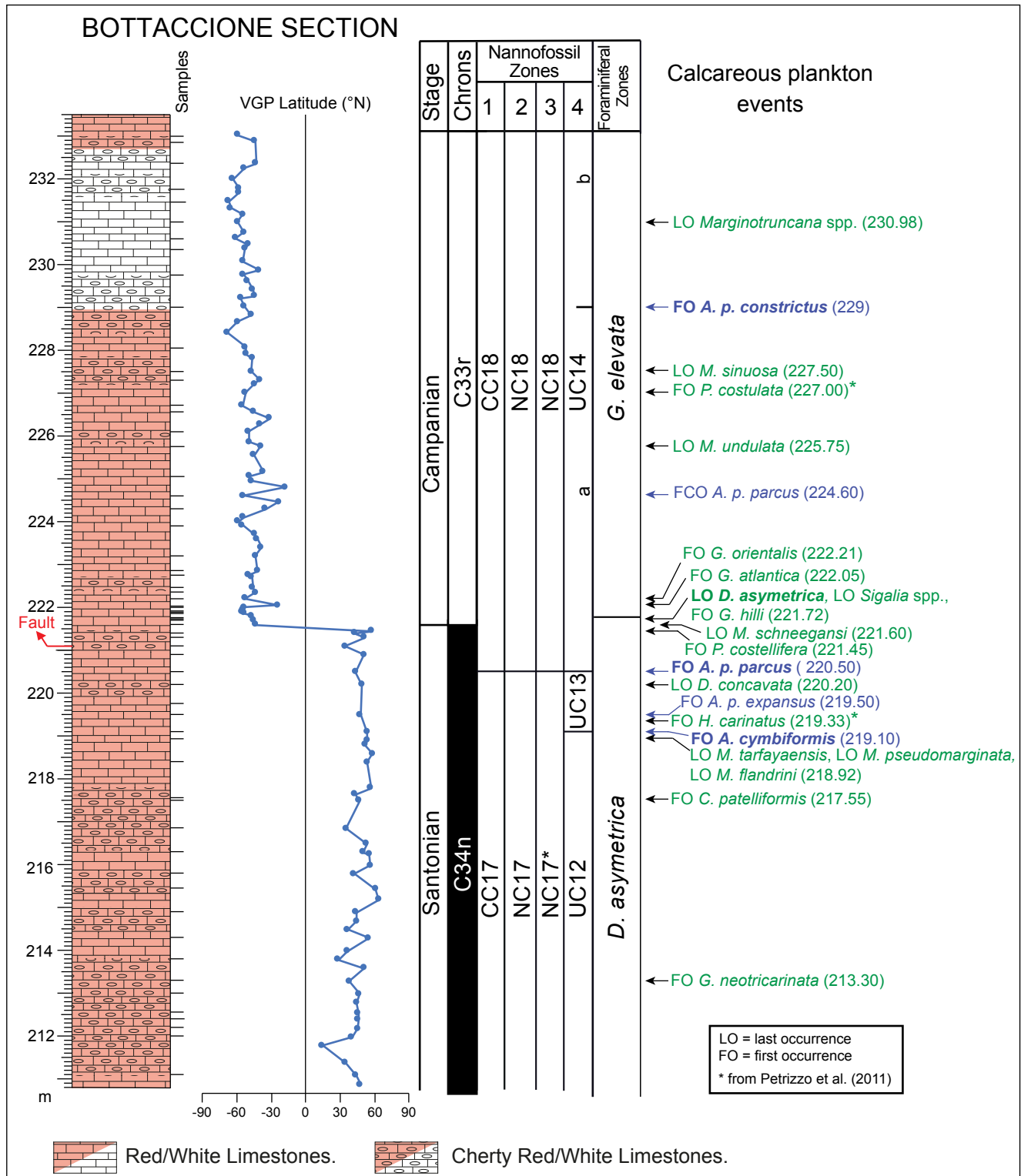


Fig. 4 - Calcareous plankton events recorded in the Bottaccione section (this study) correlated with magnetostratigraphy (Maron & Muttoni, accepted). The base of magnetochron C33r at 221.525 m is used to define the Santonian-Campanian boundary. Lithostratigraphy after Maron & Muttoni (accepted). The sample studied for calcareous plankton biostratigraphy are on the right side of the lithostratigraphic column. The calcareous nannofossil events are in blue, and the zonal marker evidenced in bold. Planktonic foraminiferal events are in green, and the zonal marker in bold. FO = first occurrence, LO = last occurrence. Events marked with an asterisk are according to Petrizzo et al. (2011).

eral increase in size (coccolith length) of *A. parvus parvus* specimens, consistently with previous records (Gardin et al. 2001; Wolfgring et al. 2018).

As far as *A. parvus expansus* is concerned, specimens in the lower part of the range (219.5–221.1 m) are rather small (coccolith length of 10–10.2 µm) and co-occur with “small” *A. parvus expansus* (coccolith length varying between 9.5 and 9.9 µm) from 220.2 m upwards. The coccolith length increases at 221.3 m as testified by presence of some relatively large specimens with length of 11–12.3 µm, together with small specimens (coccolith length varying between 9.5 and 9.9 µm) through the rest of the studied interval.

Planktonic foraminifera

The test of the specimens observed in thin section is generally well-preserved. The preservation of specimens in the washed residues varies from poor to moderate as a result of the procedure applied to process the rock samples. Planktonic foraminiferal assemblages are generally diverse and yield a typical tropical Tethyan assemblage (Suppl. Tab. 2) with unkeeled globigeriniform (genera *Whiteinella*, *Archaeoglobigerina*, *Costellagerina*, *Rugoglobigerina*), planispiral (genus “*Globigerinelloides*”) and biserial (genera *Planoheterohelix*, *Pseudotextularia* and *Pseudoguembelina*) taxa as well as abundant single- (genus *Globotruncanita*) and double-keeled (genera *Dicarinella*, *Marginotruncana*, *Contusotruncana* and *Globotruncana*) taxa. Marker and the most common species are illustrated in Plate 3.

In addition to the taxonomically well-known species, we have also found specimens that resemble the species holotypes but possess some morphological differences. For instance, specimens assigned to *Globotruncanella* cf. *petaloidea* (Suppl. Tab. 2) resemble the holotype but show a more pinched lateral profile and a slightly smaller umbilical area. These specimens are found in the Bottaccione section well below the usually documented first occurrence of *Globotruncanella petaloidea* in middle-upper Campanian (Gradstein 1978; Premoli Silva & Sliter 1995; Zepeda 1998). Further studies are needed to evaluate their taxonomic and biostratigraphic significance.

Planktonic foraminiferal assemblages from the base of the studied interval (212.20 m) to 221.45 m show a moderate preservation and are generally diverse, whereas assemblages from 221.60 to 226.10 m are less well-preserved and diverse and contain

abundant small-sized biserial and common globigeriniform taxa, while keeled specimens are rare.

The stratigraphic interval from 212.20 to 221.72 m is assigned to the *Dicarinella asymetrica* Taxon Range Zone based on the extinction of the marker species *D. asymetrica* at 221.72 m, while the overlying interval from 221.72 to 232.33 m is assigned to the *Globotruncanita elevata* Interval Zone (Fig. 3), following the subtropical biozonation by Premoli Silva & Sliter (1995) and Robaszynski & Caron (1995).

Secondary planktonic foraminiferal events identified in the *Dicarinella asymetrica* Zone are listed below in stratigraphic order from bottom to top (Fig. 3): a) the FO of *Globotruncana neotricarinata* at 213.30 m, b) the FO of *Contusotruncana patelliformis* at 217.55 m, c) the LO (last occurrence) of *Marginotruncana tarfayaensis*, *Marginotruncana pseudomarginata* and *Muricobedbergella flandrini* at 218.92 m, d) the FO of *Hendersonites carinatus* at 219.33 m, e) the LO of *Dicarinella concavata* at 220.20 m, f) the FO of *Pseudoguembelina costellifera* at 221.45 m, g) the LO of *Marginotruncana schneegansi* at 221.60 m, and h) the LO of *Sigalia* species and the FO of *Globotruncana hilli* at 221.72 m. Planktonic foraminiferal events in the *Globotruncanita elevata* Zone (Fig. 3) include: a) the FO of *Globotruncanita atlantica* at 222.05 m, b) the FO of *Globotruncanita orientalis* at 222.21 m, c) the LO of *Marginotruncana undulata* at 225.75 m, d) the FO of *Pseudoguembelina costulata* at 227.00 m, and e) the LO of *Marginotruncana sinuosa* at 227.50 m.

DISCUSSION

Calcareous plankton biostratigraphy

Calcareous nannofossil assemblages of the Santonian-Campanian interval of the Bottaccione section were investigated in the 60s and 70s (Mohler 1966; Monechi & Pirini 1975; Monechi 1977). Monechi & Thierstein (1985) established a first nannofossil biostratigraphy of the upper Campanian-lower Eocene interval of the Bottaccione section calibrated with planktonic foraminifera (Premoli Silva et al. 1977; Napoleone et al. 1983) and magnetostratigraphy (Alvarez et al. 1977). Gardin et al. (2001) revised and implemented the biostratigraphy of the Santonian-Maastrichtian interval and Tremolada (2002) focused on the upper Albian - lowermost Campanian interval, in both cases

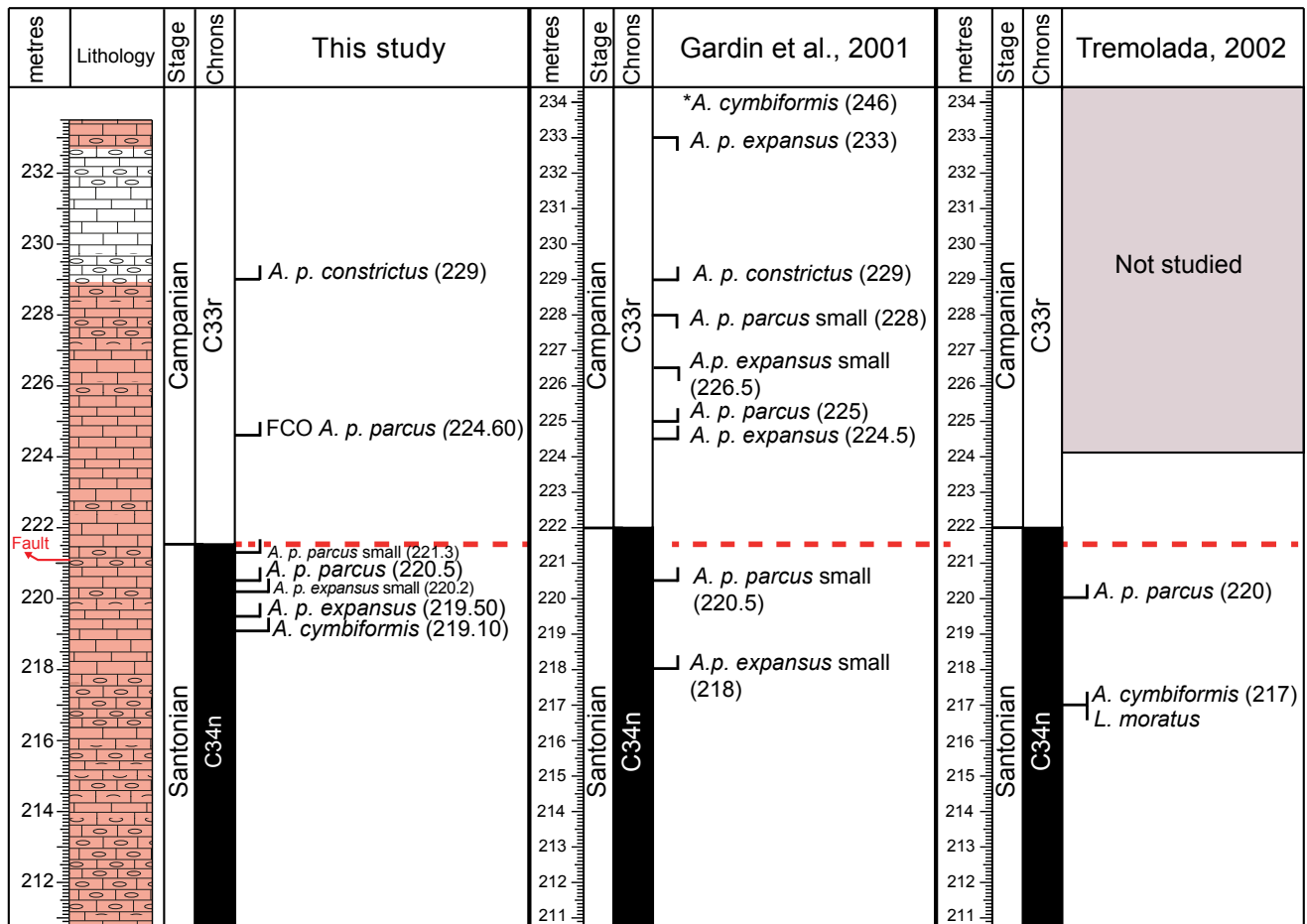


Fig. 5 - Comparison of calcareous nannofossil events found in this study and previously recorded (Gardin et al. 2001; Tremolada 2002) in the Bottaccione section. The Santonian-Campanian boundary is placed at 221.525 m according to updated magnetostratigraphy (Maron & Muttoni, accepted). The asterisk (*) added to *A. cymbiformis* was used to illustrate the FO documented at a meter level (246 m) above the studied interval.

investigating the samples previously used for planktonic foraminiferal studies by Premoli Silva & Sliter (1995).

In Fig. 5 our results are compared to the nannofossil biostratigraphies of Gardin et al. (2001) and Tremolada (2002). *Arkhangelikiella cymbiformis* (length $>8 \mu\text{m}$) was first observed at 219.10 m, while Tremolada (2002) reported the FO of this species at 217 m in the upper Santonian. Both these results differ from data by Gardin et al. (2001) who found *A. cymbiformis* in the Campanian at 246 m. The earliest species of *Aspidolithus* recorded in this study is *A. parvus expansus* (length $\geq 10 \mu\text{m}$) which occurs for the first time at 219.50 m in the uppermost Santonian. The presence of *A. parvus expansus* in the Bottaccione section was not documented by Tremolada (2002). Otherwise, Gardin et al. (2001) observed the occurrence of “small” *A. parvus expansus* at 218 m in the uppermost Santonian, and

A. parvus expansus (length $\geq 10 \mu\text{m}$) at 224.5 m in the lowermost Campanian.

The FO of *A. parvus parvus* (length $\geq 10 \mu\text{m}$) was detected at 220.5 m in the topmost Santonian, very close to the FO of *A. parvus parvus* at 220 m documented by Tremolada (2002), and at the same level of the FO of “small” *A. parvus parvus* reported by Gardin et al. (2001).

In this study, we distinguish the FO of *A. parvus parvus* (length $\geq 10 \mu\text{m}$) characterized by rare and sporadic abundance from its first common occurrence (FCO), marked by a continuous and frequent presence in the assemblage in the lowermost Campanian (224.6 m). This FCO is very close to the level where Gardin et al. (2001) placed the FO of *A. parvus parvus*.

The FO of *A. parvus constrictus* is observed at 229 m in the lower Campanian and corresponds to same level reported by Gardin et al. (2001). The

presence of “small” *A. parvus expansus*, “small” *A. parvus parvus* and “small” *A. parvus constrictus* (length <10 µm) is recorded in this study in co-occurrence with normal specimens. As discussed above, we observed a gradual minor increase in size of *Aspidolithus* specimens as also reported by Gardin et al. (2001) and Wolfgring et al. (2018).

The different positions of nannofossil events in this study relative to previous investigations of the Bottaccione section (Gardin et al. 2001; Tremolada 2002) may be ascribed to various reasons: a) the overall nannofossil abundance is low and the preservation is moderate to poor; b) both *A. cymbiformis* and *A. parvus parvus* show rare and sporadic occurrences at the beginning of their range; c) the sampling resolution applied for this study is much higher than previous investigations.

The sequence of the nannofossil events calibrated with the magnetostratigraphy at the Bottaccione section (Maron & Muttoni, accepted), from the oldest to the youngest, is as follow (Fig. 4): 1) FO *A. cymbiformis* (base of biozone UC13) in the uppermost part of 34n magnetochron; 2) FO *A. parvus expansus* in the uppermost part of magnetochron C34n; 3) FO *A. parvus parvus* (base of biozones CC18, NC18, NC*18a and UC14a) in the topmost part of magnetochron C34n; 4) FCO *A. parvus parvus* in the lowermost part of magnetochron C33r; 5) FO *A. parvus constrictus* (base of biozone UC14b) in the lower part of magnetochron C33r.

The planktonic foraminiferal biostratigraphy of the Santonian-Campanian boundary interval in the Bottaccione section was investigated several times (Premoli Silva & Sliter 1995; Petrizzo et al. 2011; Premoli Silva & Coccioni 2015). The LO of *D. asymerica* in sample 221.72 m is here identified 32 cm above the stratigraphic level reported in previous papers (Premoli Silva & Sliter 1995; Petrizzo et al. 2011; Coccioni & Premoli Silva 2015), thanks to the higher sampling resolution adopted in this study. Therefore, it falls 19.5 cm above the base of magnetochron C33r (Fig. 4). Additional bioevents that coincide with the LO of *D. asymerica* are the LO of *Sigalia* sp. and the FO of *G. hilli*. These events are followed upward by the FO of *G. atlantica* at 222.05 m and the FO of *G. orientalis* at 222.21 m in the lower part of magnetochron C33r. The top of magnetochron C34n at 221.60 m coincides with the LO of *M. schneegansi* which is preceded at 221.45 m by the FO of *P. costellifera*. Therefore, we

document a high-resolution sequence of planktonic foraminifera events across the boundary between magnetochrons C34n and C33r that allow the identification of the Santonian-Campanian boundary with a high degree of precision (Fig. 4).

The stratigraphic position of the secondary events (Fig. 4) is here revised compared to previous studies (Petrizzo et al. 2011; Coccioni & Premoli Silva 2015) with the exception of the FOs of the small-sized species *Hendersonites carinatus* and *Pseudoguembelina costulata*, as these events were detected in slightly younger stratigraphic intervals during this study (Suppl. Tab. 2), possibly as a result of the relatively poor preservation of small sized specimens in the studied samples and because of their rarity at the beginning of their stratigraphic distribution. These events are therefore placed in Fig. 4 according to Petrizzo et al. (2011).

Calcareous plankton events versus magnetostratigraphy

An integrated bio-magnetostratigraphy of the Santonian-Campanian transition (Fig. 6) has been described from the Tethys Ocean (Wolfgring et al. 2017; Wolfgring et al. 2018), Western Interior Sea (Kita et al. 2017), Poland (i.e. Dubicka et al. 2017), DSDP Site 530 (Stradner & Steinmetz 1984) and ODP Site 762 (Bralower & Siesser 1992; Petrizzo 2000).

In the Postalm section (Austrian Alps; north western Tethys), Wolfgring et al. (2018) recorded the LO of *D. asymerica* at 1.24 m above the base of magnetochron C33r and the FO *A. parvus parvus* (length ≥ 10 µm) at 1.66 m above the base of C33r, estimated to correspond to ~80 kyrs after the beginning of magnetochron C33r (Fig. 4). Other events lying close to the Santonian-Campanian boundary are the FO *C. obscurus* var. W at the top of C34n, and the FO *Ceratolithoides* cf. *C. verbeekii* in the lower C33r (Wolfgring et al. 2018). Specimens similar to *Ceratolithoides* cf. *C. verbeekii* were observed in only two samples from the Bottaccione section in the uppermost part of C34n. Regarding the planktonic foraminifera in the Postalm section Wolfgring et al. (2018) recorded the LO of *M. flandrini* at 0.64 m above the base of magnetochron C33r, whereas the species at the Bottaccione section disappears in the upper part of C34n (Fig. 6).

The FO of *A. parvus parvus* was found in the Mudurnu-Göynük area (Turkey; north-western Tethys

Postlam section (Austria) Wolfgring et al. 2018					Mudurnu-Göynük Basin (Turkey) Wolfgring et al. 2017					Bottaccione section (Italy) This Study													
Stage	Chronos	Nannofossil Zones			Foraminifera Zones	Calcareous plankton events	Stage	Chronos	Nannofossil Zones			Foraminifera Zones	Calcareous plankton events	Stage	Chronos	Nannofossil Zones			Foraminifera Zones	Calcareous plankton events			
		1	2	3					1	2	3					4	1	2			3	4	
Santonian	C34n					<i>Arkhangelskiella small</i> <i>A. cf. cymbiformis</i> <i>A. p. expansus</i> <i>C. obscurus W</i> <i>M. flandrini</i> <i>D. asymmetrica</i>	Santonian	C34n					<i>D. asymmetrica</i> <i>M. flandrini</i>	Santonian	C34n				<i>M. flandrini</i>				
	CC17																						
	NC17																						
	NC17*																						
	UC12																						
Campanian	C33r					<i>A. cf. verbeekii</i> <i>A. p. parvus</i> <i>D. asymmetrica</i> <i>M. flandrini</i> <i>G. elevata</i> <i>M. furcatus</i> <i>A. p. constrictus</i> <i>Marginotr. spp.</i>	Campanian	C33r					<i>A. p. parvus</i> <i>Marginotr. spp.</i> <i>D. asymmetrica</i>	Campanian	C33r				<i>A. p. constrictus</i>				
	CC18																						
	NC18																						
	NC18*																						
	UC14b																						
Bocieniec section (Poland) Dubicka et al. 2017					ODP Site 762C (Exmouth Plateau) Bralower & Siesser, 1992; Petrizzo, 2000					DSDP Site 530 (Angola Basin) Stradner & Steinmetz, 1984					Smoky Hill (Western Interior) Kita et al. 2017								
Stage	Chronos	Nannofossil Zones			Foraminifera Zones	Calcareous plankton events	Stage	Chronos	Nannofossil Zones			Foraminifera Zones	Calcareous plankton events	Stage	Chronos	Nannofossil Zones			Foraminifera Zones	Calcareous plankton events			
		1	2	3					4	1	2					3	4	1			2	3	4
Santonian	C34n					<i>L. septenarius</i> <i>A. cymbiformis</i> <i>C. obscurus</i> <i>Top 1st influx</i> <i>L. maleformis</i> <i>Top increase</i> <i>H. gardetiae</i> <i>O. campanensis</i> <i>D. asymmetrica</i>	Santonian	C34n					<i>D. asymmetrica</i> <i>M. flandrini</i> <i>Marginotr. spp.</i>	Santonian	C34n				<i>L. septenarius</i>				
	CC17																						
	NC17*																						
	NC17																						
	CC18																						
Campanian	C33r?					<i>L. cornuta</i> <i>W. britannica</i> <i>Marginotr. spp.</i> <i>O. campanensis big</i> <i>W. britannica</i> <i>D. concavata</i> <i>D. asymmetrica</i> <i>R. anthophorus small</i> <i>R. levis</i> <i>Z. biperforatus</i> <i>G. coronadventis</i> <i>A. p. parvus</i> <i>LO M. testudinarius</i>	Campanian	C33r					<i>G. elevata</i> <i>D. asymmetrica</i> <i>A. p. parvus</i> <i>A. p. constrictus</i>	Campanian	C33r				<i>M. furcatus</i> <i>B. hayi</i> <i>A. parvus</i>				
	CC18																						
	NC18																						
	NC18*																						
	UC14																						

Fig. 6 - Comparison of calcareous plankton events relative to magnetostratigraphy in the Bottaccione section and in other sections across the Santonian-Campanian boundary interval. Calcareous nannofossils events are in blue, planktonic foraminiferal events are in green. The base of magnetic chron C33r is used to place the base of the Campanian Stage. In the Bocieniec section the Santonian-Campanian boundary is placed according to the LO of crinoid *Marsupites testudinarius*.

ys) approximately 500 ka after the beginning of magnetic reversal C33r (Wolfgring et al. 2017) (Fig. 6). However, this taxon is rare in this composite section characterized by poorly preserved assemblages. *Dicarinella asymmetrica* is also rare and occurs discontinuous-

ly till its disappearance near the top of magnetochron C34n in a slightly older stratigraphic level than documented in the Bottaccione section. *Marginotruncana* spp. and *M. flandrini* disappear in the lower part of magnetochron C33r and in the upper part of C34n,

respectively (Fig. 6). Although the planktonic foraminifera events are recorded in the same sequence, the disappearance of *Marginotruncana* spp. is clearly older in the Turkish section compared to the Bottaccione section.

Kita et al. (2017) indicated two additional potential markers close to the Santonian-Campanian boundary: the LO *H. trabeculatus* (>7 µm) at the top of magnetochron C34n and the LO *Z. biporatus* in the lowermost C33r. In the Bottaccione section, *H. trabeculatus* specimens larger than 7 µm were not observed, whereas the presence of *Z. biporatus* was noticed only in one sample (in the lower part of C34n).

At the Exmouth plateau (ODP Hole 762C), Bralower & Siesser (1992) found the FOs *A. parvus parvus* and *A. parvus constrictus* around 2.67 meter, in the uppermost part of magnetochron C34n, while the LO *D. asymetrica* falls 0.98 m above the base of magnetochron C33r (Petruzzo 2000). Instead, *Marginotruncana* spp. and *M. flandrini* have their LOs in the upper part of magnetochron C34n. Compared to the Bottaccione section, the LOs *M. flandrini* and *D. asymetrica* do occur in equivalent stratigraphic levels, whereas the LO of *Marginotruncana* spp. is recorded in definitively older levels at Exmouth Plateau.

The results of Stradner & Steinmetz (1984) show the FO of *A. parvus* in the lower part of magnetochron C33r in the Angola Basin (DSDP Hole 530A) (Fig. 6). Stradner & Steinmetz (1984) included in *A. parvus* only specimens with a rim/central area ratio between 1 and 1.25, thus excluding potential *A. parvus parvus* specimens having a rim/central area ratio between 1.25 and 2.0 with a possible lower occurrence (Kita et al. 2017).

In the Bocieniec section (Poland), the Santonian-Campanian boundary was placed according to the LO of crinoid *Marsupites testudinarius* (Dubicka et al. 2017). The available magnetostratigraphy for this section is uncertain due to the anomalous values of the magnetic polarities. As a consequence, the boundary between magnetochrons C34n and C33r remains indefinite. According to Dubicka et al. (2017), the LO of *D. asymetrica* and the extinction of *Marginotruncana* spp. occur in the stratigraphic interval inferred to contain the boundary between magnetochrons C34n and C33r, whereas the FO *A. parvus parvus* was observed in the lower part of magnetochron C33r. In the Bocieniec section all these events (LO *D. asymetrica*; LO of *Marginotruncana* spp.; FO *A. parvus parvus*) fall above the LO of crinoid *M. testudinarius* (Fig. 4).

The comparison with available bio-magnetostratigraphic data show that the FO of *A. parvus parvus* has been found in a stratigraphic interval between the topmost part of magnetochron C34n and the lowermost part of magnetochron C33r, whereas the extinction of *D. asymetrica* is recorded slightly above the base of magnetochron C33r at all localities except for the Göynük area in Turkey where it falls at the top of magnetochron C34n. In conclusion, according to our findings, the base of magnetochron C33r lies between the FO of *A. parvus parvus* and the LO of *D. asymetrica* in the Bottaccione section and both microfossil events may be used to approximate the base of the Campanian Stage equated to the base of magnetochron C33r.

CONCLUSIONS

High-resolution calcareous nannofossil and planktonic foraminiferal biostratigraphy in the Santonian-Campanian boundary interval of the Bottaccione section results in the identification of several FO and LO directly calibrated against magnetostratigraphy. The comparison with previous data obtained for the Bottaccione section displays some discrepancies mainly due to different sampling rate, taxonomic ambiguities, general rarity and moderate to poor preservation of both nannofossil and foraminiferal assemblages. A critical review of all available calcareous plankton data directly correlated with magnetostratigraphy shows that the FO of *A. parvus parvus* is comprised within the topmost part of magnetochron C34n and the lowermost portion of magnetochron C33r, whereas the LO of *D. asymetrica* is documented in the lowermost part of magnetochron 33r, with the only exception of one section in Turkey where this datum correlates with the topmost magnetochron C34n. Adopting the base of magnetochron C33r to place the base of the Campanian stage, the FO of *A. parvus parvus* and the LO of *D. asymetrica* are proposed as the microfossil events to approximate the Santonian-Campanian boundary.

Acknowledgements: The Associate Editor Luca Giusberti, Simonetta Monechi and an anonymous Reviewer are warmly acknowledged for their constructive detailed criticism that greatly improved the quality of the manuscript. This research was funded through the "Piano di Sostegno alla Ricerca of the University of Milan". This study was partially supported by the International Subcommission on Cretaceous Stratigraphy of the International Commission on Stratigraphy (ICS).

PLATE 1

Selected calcareous nannofossil species from the Bottaccione section. For each taxon (a) cross-polarized light; (b) quartz lamina.

- 1) *Ahmuelerella regularis*, sample 213.8 m.
- 2) *Amphizygus minimus*, sample 219.75 m.
- 3) *Arkhangelskiella confusa*, sample 219.5 m.
- 4) *Arkhangelskiella cymbiformis*, sample 221.4 m.
- 5) *Aspidolithus parvus expansus* var. "small", sample 220.5 m.
- 6) *Aspidolithus parvus expansus*, sample 227.5 m.
- 7) *Aspidolithus parvus parvus* var. "small", sample 229 m.
- 8) *Aspidolithus parvus parvus*, sample 232.33 m.
- 9) *Aspidolithus parvus parvus*, sample 233 m.
- 10) *Aspidolithus parvus constrictus* var. "small", sample 230.6 m.
- 11) *Aspidolithus parvus constrictus* var. "small", sample 232.85 m.
- 12) *Aspidolithus parvus constrictus*, sample 230.6 m.
- 13) *Biscutum constans*, sample 220.9 m.
- 14) *Biscutum* sp., sample 212.40 m.
- 15) *Biscutum* sp., sample 220.2 m.
- 16) *Chiastocyclus bifarius*, sample 218.4 m.
- 17) *Cyclagelosphaera reinhardtii*, sample 221.4 m.
- 18) *Cribrosphaerella ebrenbergii*, sample 221.9 m.

PLATE 2

Selected calcareous nannofossil species from the Bottaccione section. For each taxon (a) cross-polarized light; (b) quartz lamina.

- 1) *Cylindralithus biarcus*, sample 221.9 m.
- 2) *Cylindralithus sculptus*, sample 221.9 m.
- 3) *Discorhabdus ignotus*, sample 220.9 m.
- 4) *Eiffellithus eximius*, sample 221.3 m.
- 5) *Eiffellithus gorkae*, sample 216.3 m.
- 6) *Eiffellithus nudus*, sample 222 m.
- 7) *Helicolithus trabeculatus*, sample 221.4 m.
- 8) *Lithastrinus grillii*, sample 216.85 m.
- 9) *Lucianorhabdus cayencii*, sample 214.9 m.
- 10) *Microrhabdulus decoratus*, (a) cross-polarized; (b) quartz lamina, sample 220.5.
- 11) *Micula staurophora*, (a) cross-polarized; (b) quartz lamina, sample 230.6 m.
- 12) *Quadrum gartneri*, sample 219.1 m.
- 13) *Reinhardtites anthophorus*, sample 232.85 m.
- 14) *Reinhardtites* sp., sample 218.4 m.
- 15) *Retecapsa ficula*, sample 222 m.
- 16) *Rucinolithus hayi*, sample 229.75 m.
- 17) *Rucinolithus terebrodentarius*, sample 219.5 m.
- 18) *Zenrhabdotus biperforatus*, sample 219.75 m.

PLATE 3

Selected planktonic foraminifera species from the Bottaccione section. Scale bars = 100 μ m.

- 1) *Dicarinella asymetrica*, sample 221.72 m.
- 2) *Globotruncana linneiana*, sample 212.20 m.
- 3) *Globotruncanita elevata*, sample 224.60 m.
- 4) *Contusotruncana fornicata*, sample 221.71 m.
- 5) *Globotruncana arca*, sample 223.92 m.
- 6) *Marginotruncana coronata*, sample 212.20 m.
- 7) *Marginotruncana pseudolinneiana*, sample 224.60 m.
- 8) *Marginotruncana undulata*, sample 225.75 m.
- 9) *Marginotruncana sinuosa*, sample 218.92 m.
- 10) *Marginotruncana schneegansi*, sample 217.55 m.
- 11) *Marginotruncana pseudomarginata*, sample 218.40 m.
- 12) *Globotruncana neotricarinata*, sample 221.71 m.
- 13) *Globotruncana bulloides*, sample 222.05 m.
- 14) *Globotruncanita stuartiformis*, sample 220.25 m.
- 15) *Contusotruncana patelliformis*, sample 221.71 m.
- 16) *Globotruncana orientalis*, sample 221.21 m.
- 17) *Globotruncanita atlantica*, sample 222.05 m.
- 18) *Sigalia* sp., sample 221.71 m.
- 19) *Pseudotextularia nuttalli*, sample 229.75 m.
- 20) *Ventilabrella eggeri*, sample 214.30 m.
- 21) *Globotruncana hilli*, sample 224.60 m.
- 22) "*Globigerinelloides*" *prairiehillensis*, sample 231.76.
- 23) "*Globigerinelloides*" *bollii*, sample 213.30 m.
- 24) *Laeviheterohelix pulchra*, sample 232.33 m.

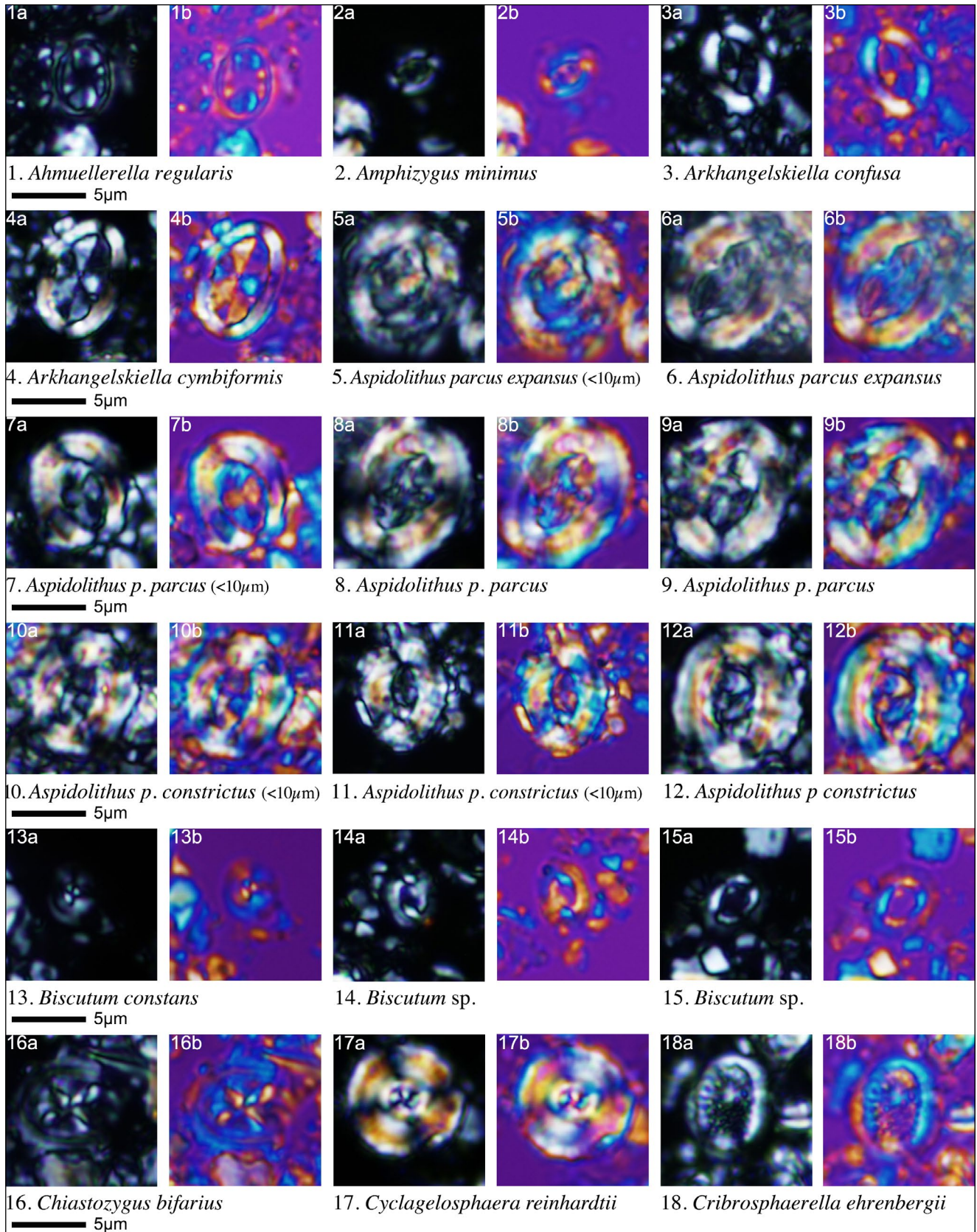
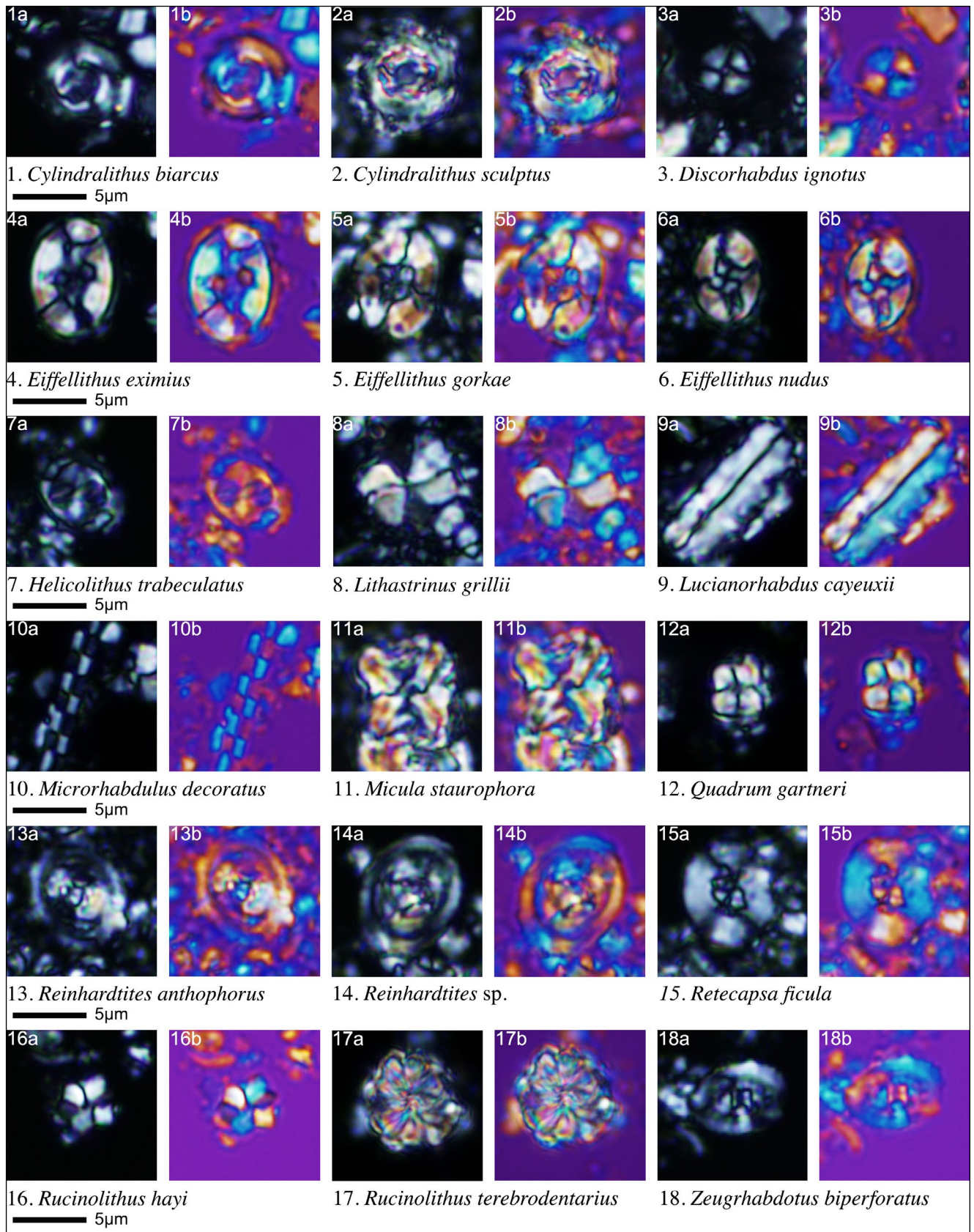


PLATE 1



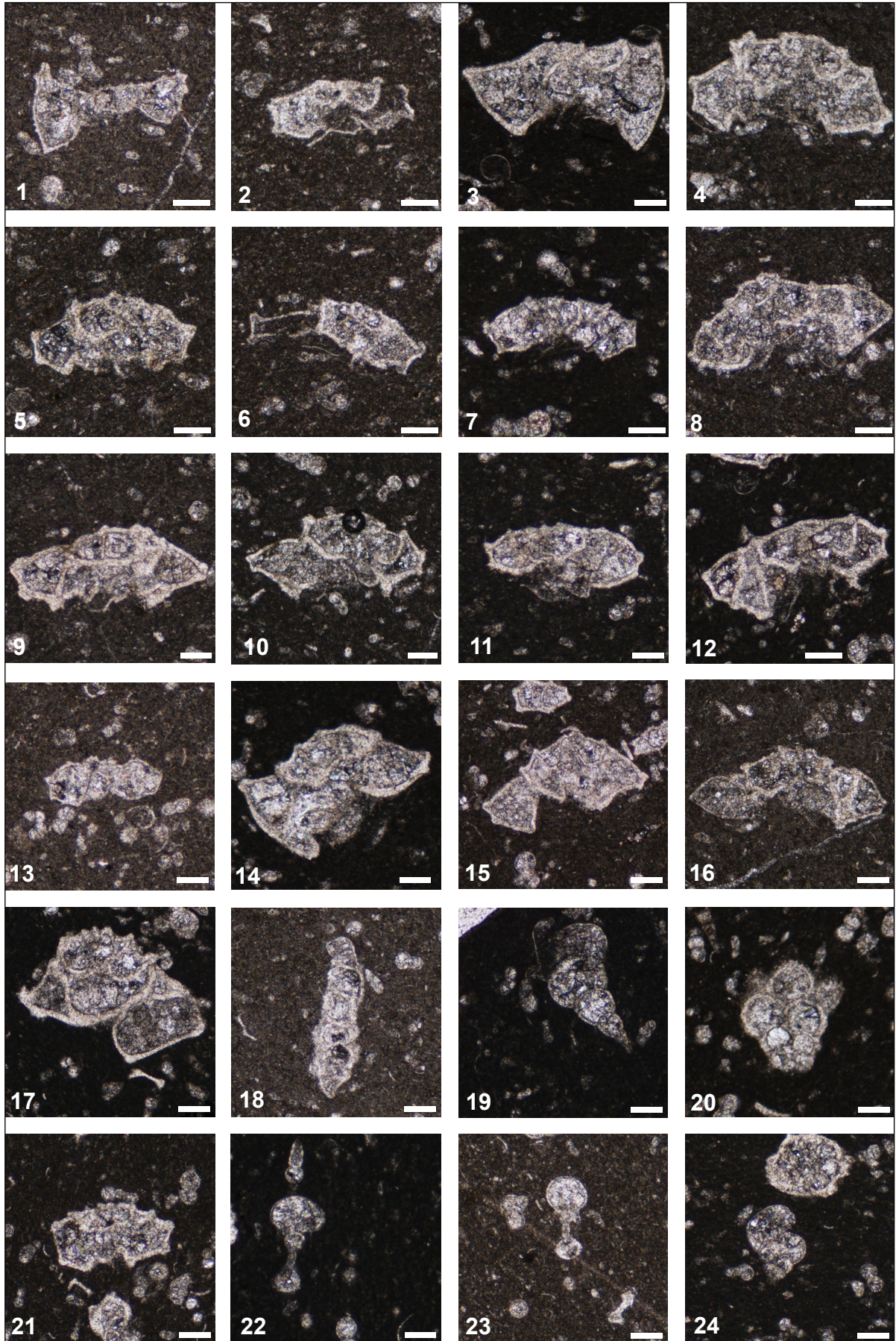


PLATE 3

APPENDIX

In this appendix we describe the diagnostic characters of the genus *Aspidolithus* and of the *Aspidolithus parvus* subspecies. The morphometric data observed in the studied interval of the Bottaccione section are also reported and compared to previous results from the Santonian-Campanian boundary interval.

Order **Arkhangelskiales** Bown & Hampton in
Young and Bown, (1997)
Family Arkhangelskiellaceae Bown & Hampton,
1997 in Bown & Young, 1997
Genus *Aspidolithus* Noël, 1969

Type-species: *Aspidolithus angustus* Noël, 1969.

Description. Elliptical coccolith with a tired bicyclic rim and a central area filled by perforated plates with axial sutures. At polarizing light microscope, the inner and outer cycles of the rim are visible in distal view, whereas in proximal view only the outer cycle is visible. At crossed nicols, the inner cycle appears brighter than the outer cycle.

Remarks. In this work, we follow Laurer (1974), Prins in Perch Nielsen (1979) and Perch-Nielsen (1985) and, accordingly, genus *Aspidolithus* is differentiated from genus *Broinsonia* due to the presence of plates instead of a cross in the central area. Within the *Aspidolithus* lineage, the subsequent appearances of *A. parvus expansus*, *A. parvus parvus* and *A. parvus constrictus* are marked by a gradual reduction of the central area/margin ratio as described by Wise (1983).

Aspidolithus parvus constrictus (Hattner et al.,
1980) Perch-Nielsen, 1984

1980 *Broinsonia parva constricta* – Hattner, Wind and Wise, p. 23; Plate 2, Figs 1-3, 5-8.

1984 *Aspidolithus parvus constrictus* – Perch-Nielsen, p. 43.

Remarks. A subspecies of *Aspidolithus parvus* with a small central area spanned by a perforated plate divided by axial sutures. One to three perforations per quadrants lie parallel to the major axis. The width of the central area is small compared to

the shield margin and have a width equivalent or less than the shield margin (b/a ratio ≤ 1). *A. parvus constrictus* evolved during the early Campanian from *A. parvus parvus* and represents the youngest subspecies in the *Aspidolithus* lineage.

Specimens with the same b/a ratio but a total length $<10 \mu\text{m}$ were considered as “small” *A. parvus constrictus* by Gardin et al. (2001). Wolfgring et al. (2018), instead, considered small the specimens with a total length $<9 \mu\text{m}$. Both papers outline an increase in size in younger levels.

In the studied Bottaccione section (this work) *A. parvus constrictus* specimens display a total length varying between 8 and $10.3 \mu\text{m}$ with no correlation with the stratigraphic position.

Aspidolithus parvus expansus (Wise and Watkins
in Wise, 1983) Perch-Nielsen, 1984

1983 *Broinsonia parva expansa* – Wise and Watkins in Wise, p. 506; plate 9, Figs. 1-5; plate 10, Figs. 5-9; Plate 11, Figs. 1-9.

1984 *Aspidolithus parvus expansus* – Perch-Nielsen, p. 43.

Remarks. A subspecies of *Aspidolithus parvus* with a wide central area spanned by a perforated plate divided by axial sutures. Central area perforations lie parallel to the ellipse axes. The width of the central area is approximately twice or more than twice the width of the shield margin (the b/a ratio is ≥ 2). *A. parvus expansus* represents the oldest subspecies belonging to the *Aspidolithus parvus* lineage starting in the late Santonian (Wise 1983; Perch-Nielsen 1985).

Specimens with this b/a ratio but a total length $<10 \mu\text{m}$ or $<9 \mu\text{m}$ were considered as “small” *A. parvus expansus* by Gardin et al (2001) and Wolfgring et al. (2018), respectively.

The specimens observed in the studied Bottaccione section have a length variable between 9 and $12.3 \mu\text{m}$. In the lowermost part of the subspecies range (latest Santonian) specimens are rather small (coccolith length of $10\text{--}10.2 \mu\text{m}$) and co-occur with “small” *A. parvus expansus* (coccolith length varying between 9 and $9.9 \mu\text{m}$) from just prior to the Santonian-Campanian boundary. The coccolith length increases in the earliest Campanian as testified by presence of some relatively large specimens (total length of $11\text{--}12.3 \mu\text{m}$) together with small specimens (length varying between 9.5 and $9.9 \mu\text{m}$) through the rest of the studied interval.

Aspidolithus parvus parvus (Stradner, 1963) Noël,
1969

1963 *Arkhangel'skiella parva* – Stradner, p. 10; Plate 1, Figs. 3, 3a.

1969 *Aspidolithus parvus* – Noël, p. 196; Plate 1, Figs. 3, 4.

Remarks. A subspecies of *Aspidolithus parvus* with a central area spanned by a perforated plate divided by axial sutures. Central area perforations lie parallel to the ellipse axes. The width of the central area is approximately between one to two times the width of the shield margin (b/a ratio between 1 and 2). In the latest Santonian, *A. parvus parvus* evolved from *A. parvus expansus* with a reduction of the central area width.

Specimens with this b/a ratio but a total length <10 µm were considered as “small” *A. parvus parvus* by Gardin et al. (2001); Wolfgring et al. (2018), instead, considered small the specimens with total

length <9 µm. Both studies outline an increase in size upwards.

In the studied Bottaccione section *A. parvus parvus* specimens have a length varying between 9.5 and 11.8 µm, with a general increase in coccolith length upwards in analogy to previous records (Gardin et al. 2001; Wolfgring et al. 2018). However, in the lowermost part of its range (latest Santonian), the coccolith length varies between 10 µm and 10.2 µm, thus, within the size range of *A. parvus parvus* (≥10 µm, following Gardin et al. 2001) although very close to the lower limit of size range. A single specimen with total length of 9.6 µm (small *A. parvus parvus*) was observed in this interval. A minor increase in length size (10.5–11.7 µm) of *A. parvus parvus* coccoliths is observed in the lower Campanian; these specimens co-occur with small *A. parvus parvus* coccoliths with length varying from 8.4 to 9.9 µm.

REFERENCES

- Almogi-Labin A., Eshet Y., Flexer A., Honigstein A., Moshkovitz S. & Rosenfeld A. (1991) - Detailed biostratigraphy of the Santonian/Campanian boundary interval in Northern Israel. *Journal of Micropalaeontology*, 10: 39-50.
- Alvarez W. & Montanari A. (1988) - The Scaglia limestone (Late Cretaceous–Oligocene) in the northeastern Apennines carbonate sequence: stratigraphic context and geological significance. In: Premoli Silva I., Coccioni R. & Montanari A. (Eds.) - The Eocene–Oligocene boundary in the Marche–Umbria basin (Italy), 1: 13-29. Industrie Grafiche F.lli Anibaldi, Ancona.
- Alvarez W., Arthur M.A., Fischer A.G., Lowrie W., Napoleone G., Premoli Silva I. & Roggenthen W.M. (1977) - Upper Cretaceous–Paleocene magnetic stratigraphy at Gubbio, Italy. Type section for the Late Cretaceous–Paleocene geomagnetic reversal time scale. *Geological Society of America Bulletin*, 88: 383-389.
- Arthur M.A. & Fischer A.G. (1977) - Upper Cretaceous–Paleocene magnetic stratigraphy at Gubbio, Italy I. Lithostratigraphy and sedimentology. *Geological Society of America Bulletin*, 88: 367-371.
- Boersma A. (1981) - Cretaceous and early Tertiary foraminifers from Deep Sea Drilling Project Leg 62 sites in the central Pacific. In: Thiede J., Valuer T.L. et al. (Eds.) - Initial Reports of the Deep Sea Drilling Project, 62: 377-396. U.S. Government Printing Office, Washington.
- Bralower T.J. & Siesser W.G. (1992) - Cretaceous calcareous nannofossil biostratigraphy of ODP Leg 122 Sites 761, 762 and 763, Exmouth and Wombat Plateaus, N.W. Australia. In: von Rad U., Haq B.U. et al. (Eds.) - Proceedings Ocean Drilling Program Scientific Results, 122: 529-556. Ocean Drilling Program, College Station, Texas.
- Bralower T.J., Leckie R.M., Sliter W.V. & Thierstein H.R. (1995) - An integrated Cretaceous microfossil biostratigraphy. In: Berggren W.A., Kent D.V., Aubry M.-P. & Hardenbol J. (Eds.) - Geochronology, Time Scales and Global Stratigraphic Correlation, 54: 65-79. Society of Economic Paleontologists and Mineralogists, Special Publication.
- Bukry D. (1969) - Upper Cretaceous coccoliths from Texas and Europe. *The University of Kansas Paleontological Contributions: Article 51 (Protista 2)*: 1-79.
- Burnett J. A. (1997) - New species and new combinations of Cretaceous nannofossils and a note on the origin of *Petrarhabdus* (Deflandre) Wise & Wind. *Journal of Nannoplankton Research*, 19: 133-146.
- Burnett J.A. (1998) - Upper Cretaceous. In: Bown P.R. (Eds.) - Calcareous Nannofossil Biostratigraphy: 132-199. Kluwer Academic Publishers, London.
- Coccioni R. & Premoli Silva I. (2015) - Revised Upper Albian–Maastrichtian planktonic foraminiferal biostratigraphy and magneto-stratigraphy of the classical Tethyan Gubbio section (Italy). *Newsletters on Stratigraphy*, 48: 47-90.
- Cresta S., Monechi S. & Parisi G. (1989) - Stratigrafia del Mesozoico e Cenozoico nell'area Umbro–Marchigiana. Memorie descrittive della Carta Geologica d'Italia 39, 185 pp.
- Crux J.A. (1982) - Upper Cretaceous (Cenomanian to Campanian) calcareous nannofossils. In: Lord A.R. (Eds.) - A Stratigraphical Index of Calcareous Nannofossils 5: 81-135. British Micropalaeontological Society Series, Chichester.
- Dubicka Z., Jurkowska A., Thibault N., Rasmjooei M.J., Wojcik K., Gorzelak P. & Felisiak I. (2017) - An integrated stratigraphic study across the Santonian/Campanian boundary at Bocieniec, southern Poland: a new boundary stratotype candidate. *Cretaceous Research*, 80: 61-85.
- Falzoni F., Petrizzo M.R., Jenkyns H.C., Gale A.S. & Tsikos H. (2016) - Planktonic foraminiferal biostratigraphy and assemblage composition across the Cenomanian–Turonian boundary interval at Clot Chevalier (Vocontian Basin, SE France). *Cretaceous Research*, 59: 69-97.
- Gardin S., Del Panta F., Monechi S. & Pozzi M. (2001) - A Tethyan reference record for the Campanian and Maastrichtian stages: The Bottaccione section (Central Italy); review of data and new calcareous nannofossil results. In: G.S. Odin (Eds.) - The Campanian–Maastrichtian Stage Boundary, 19: 745-757. Developments in Palaeontology and Stratigraphy, Elsevier.
- Gradstein F.M. (1978) - Biostratigraphy of Lower Cretaceous Blake Nose and Blake-Bahama basin foraminifers DSDP Leg 44, western north Atlantic Ocean. In: Benson W.E., Sheridan R.E. et al. (Eds.) - Initial Reports of the Deep Sea Drilling Project, 44: 663-701. U.S. Government Printing Office, Washington.
- Gradstein F.M., Ogg J.G., Schmitz M.D. & Ogg G.M. (2012) - The Geologic Time Scale 2012. Elsevier, 1144 pp.
- Hancock J.M. & Gale A.S. (1996) - The Campanian Stage. *Bulletin de l'Institut royal des Sciences naturelles de Belgique: Sciences de la Terre*, 66: 103-109.
- Hattner J.G., Wind F.H. & Wise S.W. (1980) - The Santonian–Campanian boundary: comparison of nearshore-offshore calcareous nannofossil assemblages. *Cahiers de Micropalaeontologie*, 3: 9-26.
- Haynes S.J., Huber B.T. & Macleod K.G. (2015) - Evolution and phylogeny of mid-Cretaceous (Albian–Coniacian) biserial planktic foraminifera. *Journal of Foraminiferal Research*, 45: 42-81.
- Huber B.T., Petrizzo M.R., Young J.R., Falzoni F., Gilardoni S. E., Bown P.R. & Wade B.S. (2016) - Pforams@microtax: A new online taxonomic database for planktonic foraminifera. *Micropalaeontology*, 62: 429-438.
- Kita Z.A., Watkins D.K. & Sageman B.B. (2017) - High resolution calcareous nannofossil biostratigraphy of the Santonian/Campanian Stage boundary, Western Interior Basin, USA. *Cretaceous Research*, 69: 49-55.
- Lauer G. (1975) - Evolutionary trends in the Arkhangelskiellaceae (calcareous nannoplankton) of the Upper Cretaceous of Central Oman, SE Arabia. *Archives de Sciences Genève*, 28: 259-262.
- Lirer F. (2000) - A new technique for retrieving calcareous microfossils from lithified lime deposits. *Micropalaeontology*, 46: 365-369.
- Longoria J.F. (1974) - Stratigraphic, morphologic and taxonomic studies of Aptian planktonic foraminifera. *Revista Espanola de Micropalaeontologia*, Numero Extraordinario:

5-107.

- Maron M. & Muttoni G. (accepted) - A detailed record of the C34n/C33r magnetozone boundary for the definition of the base of the Campanian Stage at the Bottaccione section (Gubbio, Italy). *Newsletters on Stratigraphy*. DOI:10.1127/nos/2020/0607.
- Masters B.A. (1977) - The neotype of *Globigerina cretacea* var. *debrionensis* Carsey. *Journal of Paleontology*, 51: 643.
- Mohler H.P. (1966) - Stratigraphische Untersuchungen in den Giswiler Klippen (Prealpes Medianes) und ihrer helvetisch-ultrahelvetischen Unterlage. *Beiträge zur Geologischen Karte der Schweiz*, 129:15-84.
- Monechi S. (1977) - Upper Cretaceous and Early Tertiary nannoplankton from Scaglia Umbra Formation (Gubbio, Italy). *Rivista Italiana di Paleontologia e Stratigrafia*, 83: 759-802.
- Monechi S. & Pirini Radrizzani C. (1975) - Nannoplankton from Scaglia Umbra Formation (Gubbio) at the Cretaceous-Tertiary boundary. *Rivista Italiana di Paleontologia e Stratigrafia*, 81: 85-96.
- Monechi S. & Thierstein H.R. (1985) - Late Cretaceous-Eocene nannofossil and magnetostratigraphic correlations near Gubbio, Italy. *Marine Micropaleontology*, 9: 419-440.
- Napoleone G., Premoli Silva I., Heller F., Cheli P., Corezzi S., & Fischer A.G. (1983) - Eocene magnetic stratigraphy at Gubbio, Italy, and its implications for Paleogene geochronology. *Geological Society of America Bulletin*, 94: 181-191.
- Nederbragt A.J. (1991) - Late Cretaceous biostratigraphy and development of Heterohelicidae (planktic foraminifera). *Micropaleontology*, 37: 329-372.
- Noël D. (1969) - *Arkhangelskiella* (coccolithes Crétacés) et formes affines du Bassin de Paris. *Revue de Micropaléontologie*, 11: 191-204.
- Perch-Nielsen K. (1979) - Calcareous nannofossils from the Cretaceous between the North Sea and the Mediterranean. *Aspekte der Kriede Europas*: Stuttgart. *IUGS Series A*, 6: 223-272.
- Perch-Nielsen K. (1984) - Validation of new combinations. *INA Newsletter*, 6: 42-46.
- Perch-Nielsen K. (1985) - Mesozoic calcareous nannofossils. In: Bolli H.M., Saunders J.B. & Perch-Nielsen K. (Eds.) - *Plankton Stratigraphy*: 329-426. Cambridge University Press.
- Petrizzo M.R. (2000) - Upper Turonian-lower Campanian planktonic foraminifera from southern mid high latitudes (Exmouth Plateau, NW Australia): biostratigraphy and taxonomic notes. *Cretaceous Research*, 21: 479-505.
- Petrizzo M.R. & Huber B.T. (2006) - Biostratigraphy and taxonomy of Late Albian planktonic foraminifera from ODP Leg 171b (western north Atlantic Ocean). *Journal of Foraminiferal Research*, 36: 165-189.
- Petrizzo M.R., Falzoni F. & Premoli Silva I. (2011) - Identification of the base of the lower-to-middle Campanian *Globotruncana ventricosa* Zone: Comments on reliability and global correlations. *Cretaceous Research*, 32: 387-405.
- Petrizzo M.R., Berrocoso A.J., Falzoni F., Huber B.T. & Macleod K.G. (2017) - The Coniacian-Santonian sedimentary record in southern Tanzania (Ruvuma Basin, East Africa): Planktonic foraminiferal evolutionary, geochemical and palaeoceanographic patterns. *Sedimentology*, 64: 252-285.
- Premoli Silva I. (1977) - Upper Cretaceous-Paleocene magnetic stratigraphy at Gubbio, Italy II. Biostratigraphy. *Geological Society of America Bulletin*, 88: 371-374.
- Premoli Silva I. & Sliter W.V. (1995) - Cretaceous planktonic foraminiferal biostratigraphy and evolutionary trends from the Bottaccione section, Gubbio, Italy. *Palaeontographia Italica*, 82: 1-85.
- Robaszynski F. & Caron M. (1995) - Foraminifères planctoniques du Crétacé: commentaire de la zonation Europe-Méditerranée. *Bulletin de la Société Géologique de France*, 166: 681-692.
- Roth P.H. (1978) - Cretaceous nannoplankton biostratigraphy and oceanography of the northwestern Atlantic Ocean. In: Benson W.E., Sheridan R.E. et al. (Eds.) - *Initial Reports of the Deep Sea Drilling Project 44*: 663-701. U.S. Government Printing Office, Washington.
- Sissingh W. (2007) - Biostratigraphy of Cretaceous calcareous nannoplankton. *Netherlands Journal of Geosciences/Geologie en Mijnbouw*, 56: 37-65.
- Stradner H. & Steinmetz J. (1984) - Cretaceous calcareous nannofossils from the Angola Basin, Deep Sea Drilling Project Site 530. In: Hay W.W., Sibuet J.-C et al. (Eds.) - *Initial Reports of the Deep Sea Drilling Project 75*: 565-649. U.S. Government Printing Office, Washington.
- Tremolada F. (2002) - Aptian to Campanian calcareous nannofossils biostratigraphy from the Bottaccione section, Gubbio, central Italy. *Rivista Italiana di Paleontologia e Stratigrafia*, 108: 441-456.
- Wise S.W. (1983) - Mesozoic and Cenozoic calcareous nannofossils recovered by deep sea drilling project Leg 71 in the Falkland Plateau region, south-west Atlantic Ocean. In: Ludwig W.J., Krashenikov V.A. et al. (Eds.) - *Initial Reports of the Deep Sea Drilling Project 71*: 481-550. U.S. Government Printing Office, Washington.
- Wolfgring E., Wagreich M., Dinarès-Turell J., Gier S., Böhm K., Sames B., Spötl C. & Popp F. (2018) - The Santonian-Campanian boundary and the end of the Long Cretaceous Normal Polarity-Chron: isotope and plankton stratigraphy of a pelagic reference section in the NW Tethys (Austria). *Newsletter on Stratigraphy*, 51: 445-476.
- Verbeek J.W. (1977) - Calcareous nannoplankton biostratigraphy of Middle and Upper Cretaceous deposits in Tunisia, southern Spain and France. *Utrecht Micropaleontological Bulletin*, 16: 1-157.
- Wolfgring E., Wagreich M., Dinarès-Turell J., Yilmaz I.O., Böhm K. (2017) - Plankton biostratigraphy and magnetostratigraphy of the Santonian-Campanian boundary interval in the Mudurnu-G.ynük Basin, northwestern Turkey. *Cretaceous Research*, 87: 296-311.
- Zepeda M.A. (1998) - Planktonic foraminiferal diversity, equitability and biostratigraphy of the uppermost Campanian-Maastrichtian, ODP leg 122, hole 762C, Exmouth Plateau, NW Australia, eastern Indian Ocean. *Cretaceous Research*, 19: 117-152.

